


 Cite this: *RSC Adv.*, 2021, **11**, 9057

## Calycindaphines A–J, *Daphniphyllum* alkaloids from the roots of *Daphniphyllum calycinum*†

 Ji Yang,<sup>a</sup> Xin Liu,<sup>ab</sup> Jing Fu,<sup>a</sup> Hao-Yuan Lyu,<sup>a</sup> Li-Ping Bai,<sup>a</sup> Zhi-Hong Jiang<sup>id</sup>\*<sup>a</sup> and Guo-Yuan Zhu<sup>id</sup>\*<sup>a</sup>

Ten new *Daphniphyllum* alkaloids, calycindaphines A–J (1–10), together with seventeen known alkaloids were isolated from the roots of *Daphniphyllum calycinum*. Their structures were established by extensive spectroscopic methods and compared with data from literature. Compound **1** is a novel alkaloid with a new rearrangement C<sub>22</sub> skeleton with the 5/8/7/5/5 ring system. Compound **2** represents the second example of calyciphylline G-type alkaloids. Compound **10** is the first example of secodaphniphylline-type alkaloid absent of the oxygen-bridge between C-25/C-29. The possible biogenetic pathways of **1** and **2** were also proposed. All the isolated compounds were evaluated for their bioactivities in three cell models. Compounds **22**, **23**, and **26** showed significant NF-κB transcriptional inhibitory activity at a concentration of 50 μM. Compounds **16** and **18** exhibited significant TGF-β inhibitory activity in HepG2 cells. Compounds **24** and **26** induced autophagic puncta and mediated the autophagic marker LC3-II conversion in HEK293 cells.

 Received 6th January 2021  
 Accepted 22nd February 2021

DOI: 10.1039/d1ra00107h

[rsc.li/rsc-advances](http://rsc.li/rsc-advances)

### Introduction

The *Daphniphyllum* alkaloids were characteristically distributed in plants of the *Daphniphyllum* family.<sup>1–4</sup> To date, more than 200 *Daphniphyllum* alkaloids with nearly 20 skeletons have been isolated from ten species. *Daphniphyllum* alkaloids not only provided abundant structural types but also enlighten novel strategies for the total synthesis and biosynthesis of unusual skeletons.<sup>5–10</sup> *Daphniphyllum calycinum*, an evergreen tree native to southern China, provided an abundant resource of *Daphniphyllum* alkaloids.<sup>11,12</sup> The leaves, stems, and roots of *D. calycinum* are used in Traditional Chinese Medicine to treat several symptoms including fever, asthma, inflammation, and influenza.<sup>11–13</sup> Previous phytochemical investigations on the leaves and stems of *D. calycinum* led to the isolation of more than 50 *Daphniphyllum* alkaloids with 15 different skeletons. However, the chemical from the roots of the *D. calycinum* has not been reported. To seek potential bioactive alkaloids from *D. calycinum*, the roots of *D. calycinum* were first deeply studied. As a result, ten new *Daphniphyllum* alkaloids, named calycindaphines A–J (1–10), as well as 17 known alkaloids (11–27) were

isolated from the roots of *D. calycinum*. In this paper, we reported the isolation, structural elucidation, and bioactivities of these isolates.

### Results and discussion

Compound **1**, a white amorphous powder, has a molecular formula of C<sub>23</sub>H<sub>31</sub>O<sub>3</sub>N as established by its HRESIMS data (*m/z* 370.2375 [M + H]<sup>+</sup>, calcd for 370.2377), with 9 degrees of unsaturation. IR absorptions implied the presence of an ester carbonyl (1733 cm<sup>-1</sup>) and a lactam (1644 cm<sup>-1</sup>).<sup>14</sup> The <sup>1</sup>H NMR data (Table 1) of **1** exhibited proton resonances of a methoxy (δ<sub>H</sub> 3.61, s), a methyl singlet (δ<sub>H</sub> 1.10, s), a methyl doublet (δ<sub>H</sub> 1.15, d, *J* = 6.7 Hz), an olefinic proton (δ<sub>H</sub> 5.42, d, *J* = 5.2 Hz). Its <sup>13</sup>C NMR, DEPT, and HSQC spectra showed the occurrence of 23 carbon resonances (Table 2), which consisted of three methyls (a methoxy at δ<sub>C</sub> 50.9), nine methylenes (two *N*-methylenes at δ<sub>C</sub> 46.8 and 52.5), five methines (an olefinic methine at δ<sub>C</sub> 118.9), six quaternary carbons (two carbonyls at δ<sub>C</sub> 182.9 and 175.2, and three olefinic quaternary carbons at δ<sub>C</sub> 140.6, 139.0, and 135.5). The above-mentioned spectroscopic data suggested that **1** possesses two carbonyls and two double bonds which accounting for four out of nine indices of hydrogen deficiency, and the remaining five degrees of unsaturation were speculated for the presence of a pentacyclic system in **1**. The <sup>1</sup>H–<sup>1</sup>H COSY spectrum of **1** suggested three proton-bearing structural moieties: C-4/C-3/C-2/C-18/C-19/20, C-7/C-1/C-12/C-11, and C-13/C-14/C-15/C-16/C-17 (Fig. 2). These three fragments, quaternary carbons, and the nitrogen atom were then connected by the detailed HMBC analysis (Fig. 2). The HMBC correlations from

<sup>a</sup>State Key Laboratory of Quality Research in Chinese Medicine, Guangdong-Hong Kong-Macao Joint Laboratory of Respiratory Infectious Disease, Macau Institute for Applied Research in Medicine and Health, Macau University of Science and Technology, Macau, People's Republic of China. E-mail: zhjiang@must.edu.mo; gyzhu@must.edu.mo

<sup>b</sup>Biology Institute, Qilu University of Technology (Shandong Academy of Sciences), Jinan 250103, China

† Electronic supplementary information (ESI) available. See DOI: 10.1039/d1ra00107h



Table 1 <sup>1</sup>H NMR (600 MHz) spectroscopic data of compounds 1–10 in CDCl<sub>3</sub>

No.	1	2	3	4	5	6	7	8	9	10
1										
2a	2.24 (m)		2.15 (m)	3.80 (d, 4.2)	3.59 (m)	1.40 (m)	1.69 (m)	3.03 (s)	2.99 (s)	3.11 (s)
2b				2.65 (m)		0.84 (m)	1.32 (m)	1.03 (m)	0.96 (m)	1.09 (m)
3a	2.51 (m)	2.00 (m)	2.03 (m)	2.06 (m)	1.60 (m)	1.70 (m)	1.50 (m)	1.89 (m)	1.55 (m)	1.50 (m)
3b	1.94 (m)	1.66 (dd, 14.4, 4.4)	1.74 (m)	1.66 (m)	2.00 (m)	1.42 (m)		1.40 (m)	1.67 (m)	1.29 (m)
4a	2.02 (m)	4.07 (dd, 10.5, 4.4)	3.22 (t, 3.1)	2.00 (m)	1.61 (m)	1.83 (m)	1.81 (m)	1.17 (m)	1.60 (m)	1.59 (m)
4b	1.63 (m)			1.42 (m)	1.76 (m)	1.35 (m)	1.38 (m)		1.60 (m)	1.15 (m)
6		2.01 (m)	2.55 (m)	2.79 (m)	2.38 (m)			1.91 (t, 5.3)	1.99 (t, 5.3)	1.91 (t, 5.1)
7a	4.32 (t, 13.1)	2.88 (dd, 14.2, 8.9)	3.40 (dd, 14.3, 9.8)	4.98 (m)	3.36 (dd, 13.6, 10.1)	2.78 (m)	5.97 (s)	2.30 (d, 5.9)	2.60 (t, 4.6)	2.56 (d, 3.5)
7b	2.48 (m)		3.14 (m)		3.73 (dd, 13.6, 8.2)					
9								1.72 (m)	1.75 (m)	1.03 (t, 3.4)
10				2.54 (m)						
11a	5.32 (d, 5.2)	2.42 (m)	2.17 (m)	1.83 (m)	2.24 (m)	1.97 (m)	2.55 (dd, 12.9, 5.8)	1.65 (m)	1.68 (m)	1.67 (m)
11b		1.99 (m)		1.29 (m)		1.74 (m)	2.21 (m)	1.48 (m)	1.55 (m)	1.49 (m)
12a	2.67 (m)	2.01 (m)	1.90 (m)	2.07 (m)	1.60 (m)	2.31 (m)	2.38 (m)	1.59 (m)	1.79 (m)	1.59 (m)
12b	1.97 (m)	1.61 (m)	1.61 (m)	1.87 (m)	2.24 (m)	1.97 (m)		1.40 (m)	1.61 (m)	1.41 (m)
13a	3.45 (m)	2.79 (m)	2.53 (m)	1.84 (m)	2.31 (m)	2.65 (dd, 13.8, 7.9)	2.27 (m)	2.04 (m)	1.65 (m)	1.69 (m)
13b	2.89 (d, 15.5)	2.35 (m)	2.28 (dd, 13.5, 8.8)	1.68 (m)	2.61 (m)	2.30 (m)	2.07 (m)	1.96 (m)	2.86 (m)	1.54 (m)
14a	3.18 (t, 7.6)	2.93 (m)	3.18 (m)	2.74 (m)	3.27 (dt, 11.3, 8.1)	3.41 (dt, 12.2, 7.0)	3.61 (m)	2.92 (m)	2.86 (m)	1.30 (m)
14b		2.93 (m)	3.62 (m)	5.48 (m)	3.38 (m)	2.78 (m)	2.75 (q, 8.0)	1.28 (m)	2.65 (m)	1.41 (m)
15b								1.78 (m)	1.69 (m)	1.67 (m)
16a	1.80 (m)	1.79 (m)	1.83 (m)	2.18 (m)	1.22 (m)	1.78 (m)	2.29 (m)	1.73 (m)	1.73 (m)	1.75 (m)
16b	1.00 (m)	1.17 (m)	1.17 (m)	1.17 (m)	1.88 (dt, 12.1, 6.8)	1.48 (m)	2.05 (m)	1.44 (m)	1.46 (m)	1.45 (m)
17a	2.68 (m)	2.53 (m)	2.49 (m)	2.09 (m)	2.21 (m)	2.35 (m)	5.54 (m)	1.66 (m)	1.69 (m)	1.47 (m)
17b	2.46 (m)	2.23 (m)	2.21 (m)	1.42 (m)	2.46 (m)	1.90 (m)		1.54 (m)	1.56 (m)	1.16 (m)
18	2.49 (m)	2.28 (m)	2.35 (t, 6.3)	1.42 (m)	2.24 (m)	2.15 (m)	2.15 (m)	1.49 (m)	1.47 (m)	1.51 (m)
19a	3.32 (d, 9.4)	3.22 (m)	4.42 (s)		2.29 (dd, 13.6, 8.6)	4.04 (dd, 13.1, 7.9)	4.37 (dd, 13.2, 5.6)	0.90 (d, 6.5)	0.91 (d, 6.5)	0.94 (d, 6.5)
19b	3.27 (d, 9.4)	2.02 (m)			4.46 (dd, 13.6, 7.7)	3.89 (dd, 13.1, 8.9)	2.31 (m)			
20	1.15 (d, 6.7)	1.02 (d, 7.1)	1.13 (d, 6.7)	1.49 (s)	0.99 (d, 6.7)	0.93 (d, 6.9)	0.87 (d, 6.8)	0.89 (d, 6.5)	0.90 (d, 6.5)	0.89 (m)
21a	1.10 (s)	1.22 (s)	0.97 (s)	1.47 (s)	1.16 (s)	1.22 (s)	1.08 (s)	0.78 (s)	3.72 (d, 10.6)	0.76 (s)
21b									3.49 (d, 10.6)	
22								3.94 (m)		1.68 (m)
23	3.61 (s)	3.61 (s)	3.62 (s)		3.65 (s)	3.70 (s)	3.68 (s)			
24			3.25 (s)							
25a								0.59 (s)	0.78 (s)	0.89 (s)
25b								3.58 (dd, 11.8, 1.5)	4.25 (d, 12.1)	3.65 (m)
26								3.51 (d, 11.8)	3.52 (d, 12.1)	3.49 (d, 10.3)
27a								4.49 (d, 6.0)	4.66 (d, 6.9)	3.74 (dd, 11.2, 4.0)
27b								2.07 (m)	2.07 (m)	1.74 (m)
28a								1.96 (m)	1.03 (m)	1.50 (m)
28b								2.05 (m)	2.07 (m)	1.76 (m)
30								1.83 (m)	1.87 (m)	1.47 (m)
								1.47 (s)	1.43 (s)	1.20 (s)

Table 2  $^{13}\text{C}$  NMR (150 MHz) spectroscopic data of compounds 1–10 in  $\text{CDCl}_3$ 

No.	1	2	3	4	5	6	7	8	9	10
1	182.9	73.6	98.7	63.6	174.4	175.7	175.6	48.2	48.6	47.7
2	46.3	220.8	45.5	47.8	72.9	32.3	32.3	42.7	42.6	42.6
3	30.2	33.3	23.5	22.9	37.1	26.2	23.0	20.8	20.0	20.7
4	41.6	79.1	82.8	27.3	42.7	48.3	40.0	39.2	32.3	39.1
5	42.9	51.0	45.9	84.2	57.1	41.9	40.7	36.9	41.7	36.7
6	46.5	36.0	39.1	33.9	40.0	53.5	130.6	47.8	45.7	47.6
7	46.8	44.5	44.7	47.1	50.9	176.9	126.9	60.1	59.7	59.8
8	140.6	60.6	34.1	49.0	41.8	62.9	65.5	36.9	45.7	37.2
9	135.5	143.1	143.2	143.0	139.1	96.0	97.2	53.9	52.8	54.2
10	139.0	136.4	135.0	44.7	133.5	84.7	145.9	50.5	50.5	50.6
11	118.9	26.3	25.9	25.4	24.5	32.5	31.3	39.9	39.4	40.0
12	33.7	27.0	22.9	21.2	25.5	24.1	27.8	22.9	23.2	23.0
13	42.1	33.7	38.2	23.1	34.8	31.5	31.1	25.0	25.8	36.2
14	46.7	55.1	42.8	26.4	42.0	43.2	43.7	30.1	34.1	20.7
15	54.2	43.0	54.5	124.8	52.9	54.0	56.8	30.8	29.7	30.6
16	28.4	28.6	28.5	31.0	28.5	20.2	31.4	26.8	26.7	26.9
17	38.9	42.5	42.6	34.5	42.1	34.8	130.9	36.3	36.2	36.3
18	28.1	43.8	36.3	77.3	38.4	33.8	28.8	28.8	28.7	28.8
19	52.5	54.2	96.5	174.4	52.4	45.1	51.9	21.2	21.0	21.0
20	13.3	11.8	10.8	20.5	18.1	26.1	20.4	21.1	21.0	21.0
21	33.3	19.1	20.6	19.7	25.0	21.4	22.9	21.3	66.2	21.1
22	175.2	176.3	176.5	170.8	176.1	174.1	174.4	75.5	213.0	52.2
23	50.9	51.0	51.1		51.3	51.7	51.5	39.2	49.8	43.8
24			50.4					14.8	17.7	10.7
25								67.6	65.4	72.0
26								80.0	81.0	76.7
27								25.0	24.6	28.7
28								33.6	33.8	40.7
29								105.1	105.3	73.9
30								23.8	23.7	23.9

H-13/H-14 to C-8/C-9/C-22, H-16 to C-9/C-10, H-17 to C-9/C-10/C-11, H-11 to C-10/C-17, and H-23 to C-22, led to the assignment of rings A and B. Moreover, HMBC cross-peaks from H-21 to C-4/C-5/C-6/C-8 and H-6 to C-4/C-5/C-8 indicated the presence of C-5/C-6/C-8 linkage which form a seven-membered ring (ring C). HMBC correlations from H-2/H-7/H-19 to C-1, H-3/H-4/H-6 to C-5, H-7 to C-5/C-19, and H-19 to C-7 established the connectivity of rings D and E. Thus, the planar structure of **1** was assigned as shown in Fig. 2. Compound **1** has a fused 5/8/7/5/5 ring system, which contains a 1-azabicyclo[5.2.1]decane ring (rings D/E) with a ketone at C-1 and two methyls at C-18 and C-2, a cyclohepta-1,3-diene ring (ring C) with two double bonds between C-8/C-9 and C-10/C-11, and a bicyclo[3.3.0]octane ring (rings A/B) with a methoxy carbonyl at C-14 as shown in Fig. 2. Comparing with the literature, the ring system of **1** was the same as those of daphhimalenine A.<sup>14</sup> However, compound **1** possesses C<sub>22</sub> carbon skeleton like most of *Daphniphyllum* alkaloids, while daphhimalenine A loses C-21 methyl to form a C<sub>21</sub> carbon skeleton. The  $^3J_{\text{H-13a/H-14}} = 7.5$  Hz suggest that H-15/H-14 of **1** was  $\alpha$ -orientation and same as that of daphhimalenine A.<sup>14</sup> Based on the same biosynthetic origin as *Daphniphyllum* alkaloids, the configuration of H-6 was identified as  $\beta$ -orientation.<sup>11,13</sup> The relative configurations of C-20, C-21, and C-2–C-3 bond was dissented as  $\beta$ -orientation by the key NOESY correlations (Fig. 3) from H-21 to H-6/H-13b and H-20 to H-3 as well as the comparison with the literature.<sup>14</sup> To determine the

absolute configuration of **1**, the calculated ECD were performed using the time-dependent density functional theory at the PBE0-D3(BJ)/def2-SVP level for (2*R*,5*S*,6*S*,14*R*,15*R*,18*S*)-**1** and (2*S*,5*R*,6*R*,14*S*,15*S*,18*R*)-**1**. The ECD curve of **1** showed a negative Cotton effect at 217 (–51.89) nm, which was consistent with the calculated ECD spectrum of (2*R*,5*S*,6*S*,14*R*,15*R*,18*S*)-**1** (Fig. 4). Accordingly, the absolute configuration of **1** was determined as 2*R*,5*S*,6*S*,14*R*,15*R*,18*S*. The structure of **1** was thereby established (Fig. 1) and named calycindaphine A.

In the early report, the possible biogenetic pathway of daphhimalenine A was proposed that its precursor daphhimalenine B underwent multi-step oxidation to lose the C-21 and rearranged to form 1-azabicyclo[5.2.1]decane ring system.<sup>14</sup> Calycindaphine A (**1**) has the same ring system with daphhimalenine A but reserving the key C-21 methyl. According to the structure of **1**, another possible biogenetic pathway to form 1-azabicyclo[5.2.1]decane ring system was proposed, and shown in Scheme 1. The biogenetic origin of **1** and daphhimalenine A seems to be modified from a yuzurimine-type alkaloid, yunnandaphnine A (**13**).<sup>7</sup> Yunnandaphnine A might undergo the oxidation of C-1 and the breakdown of C-1/C-8 bond to form 1-azabicyclo[5.2.1]decane ring. Then, the intermediate I should undergo the dehydrogenation and sigmatropic rearrangement procedures to yield **1** (C<sub>22</sub> skeleton). The C-21 methyl of **1** should further be oxidated to give II. Then the oxidative



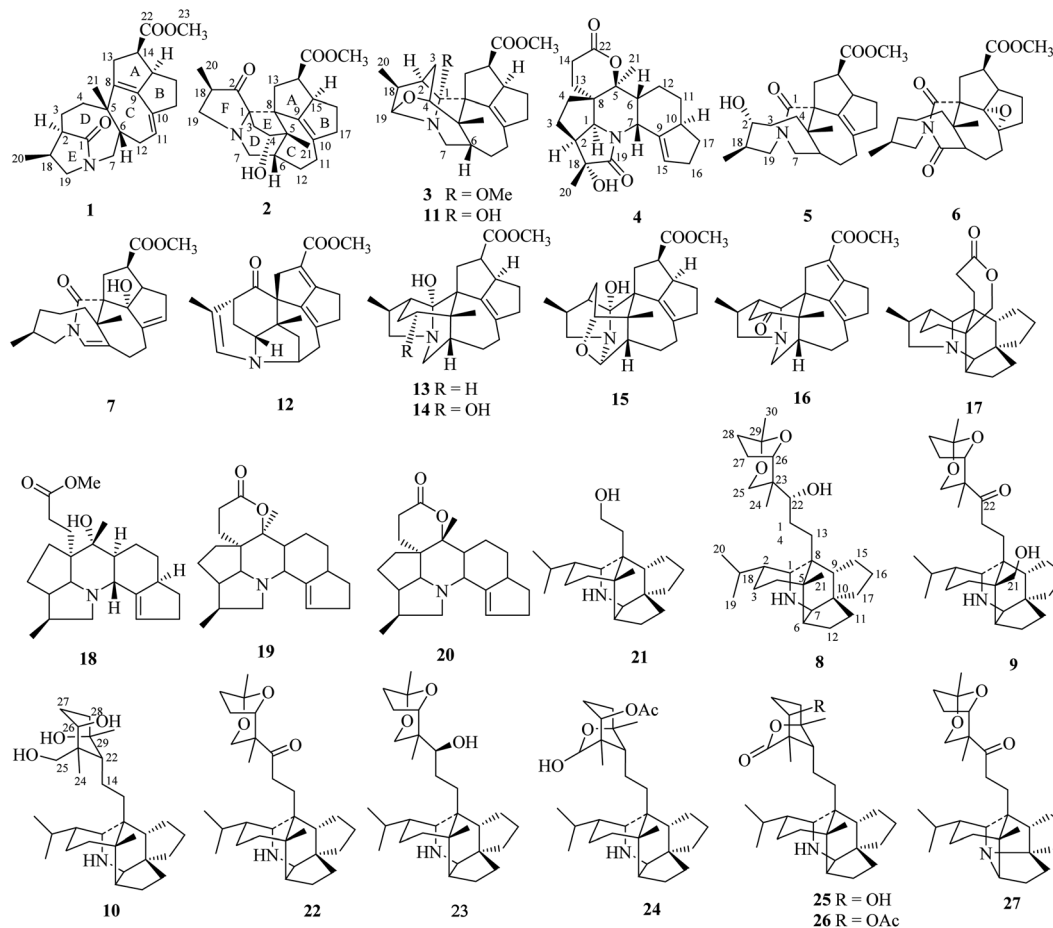


Fig. 1 Chemical structures of compounds 1–27.

decarboxylation and sigmatropic rearrangement of II afford daphhimalenine A (C<sub>21</sub> skeleton).

Compound 2 was isolated as a white amorphous powder. The molecular formula of 2 was assigned as C<sub>23</sub>H<sub>31</sub>O<sub>4</sub>N based on the quasi-molecular ion peak at *m/z* 386.2324 [M + H]<sup>+</sup> in its HRESIMS spectrum, requiring nine indices of hydrogen deficiency. The <sup>1</sup>H NMR spectrum (Table 1) of 2 revealed a methoxy ( $\delta_{\text{H}}$  3.61, s), a methyl singlet ( $\delta_{\text{H}}$  1.22, s), a methine doublet ( $\delta_{\text{H}}$  1.02, d, *J* = 7.1 Hz), an oxidized methine ( $\delta_{\text{H}}$  4.07, dd, *J* = 10.5, 4.4 Hz). The <sup>13</sup>C, DEPT, and HSQC spectra of 2 described 23 carbon resonances constituting with three methyls (a methoxy at  $\delta_{\text{C}}$  51.0), eight methylenes (two *N*-methylenes at  $\delta_{\text{C}}$  54.3 and 44.5), five methines (an oxidized methine at  $\delta_{\text{C}}$  79.2) and seven quaternary carbons (a carbonyl at  $\delta_{\text{C}}$  220.8, an ester carbonyl at  $\delta_{\text{C}}$  176.3, a couple of double bond carbons at  $\delta_{\text{C}}$  143.1 and 136.4, and an *O/N*-quaternary carbon at  $\delta_{\text{C}}$  73.6), shown in Table 2. Comparing with the known *Daphniphyllum* alkaloids, the spectroscopic data of 2 is similar to those of calyciphylline G<sup>15</sup> except for the absence of  $\Delta_{2,18}$  and  $\Delta_{19,N}$  and the presence of additional carbonyl and hydroxyl groups at C-2 and C-4, respectively. These function groups were assigned by the HMBC correlations from H-3/H-18/H-19/H-20 to C-2 and H-3/H-6/H-21 to C-4 as well as the chemical shift of C-4 (Fig. 2). The relative stereochemistry of 2 was elucidated by the NOESY experiment.

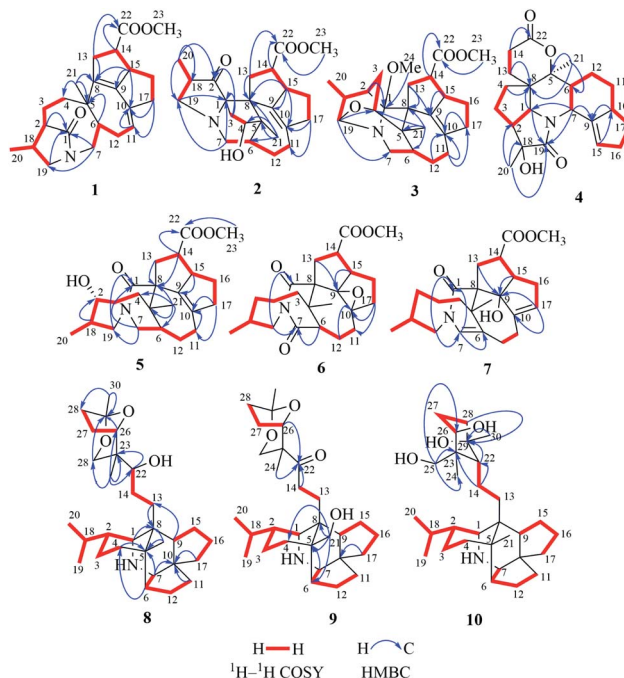


Fig. 2 Key <sup>1</sup>H–<sup>1</sup>H COSY and HMBC correlations of compounds 1–10.



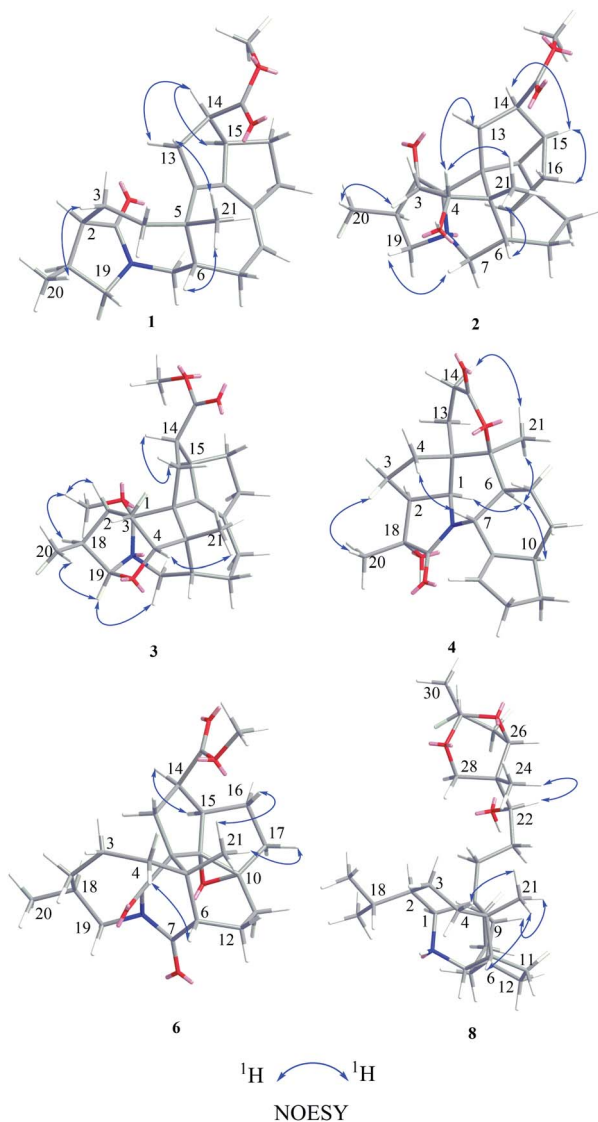


Fig. 3 Key NOESY correlations of compounds 1–4, 6, and 8.

The correlations of H-4/H-21/H-13b and H-21/H-6 suggested that they are on the same side and  $\beta$ -oriented (Fig. 3), which is the same as those of calyciphylline G.<sup>15</sup> Accordingly, the hydroxyl group at C-4 was placed at  $\alpha$ -orientation. Thus, the structure of 2 was determined as shown in Fig. 1 and named calycindaphine B.

The calyciphylline G was isolated as a quaternary amine alkaloid containing a 5-azatricyclo[6.2.1.0<sub>1,5</sub>]undecane ring in 2007.<sup>15</sup> However, the possible biogenetic pathway of this unprecedented fused-hexacyclic skeleton has not been described. Comparison of the structural features of calyciphylline G and 2 suggested that the calyciphylline G might be regarded as the key intermediate for 2. A plausible biogenetic pathway for this fused-hexacyclic skeleton is proposed as shown in Scheme 1. Calycindaphine B (2) and calyciphylline G might also be generated from yunnandaphnine A,<sup>7</sup> which might be dehydrated in ring E to form intermediated III. Then, the intermediated III should be reduced and undergo the Wagner–Meerwein rearrangement to yield calyciphylline G. Following,

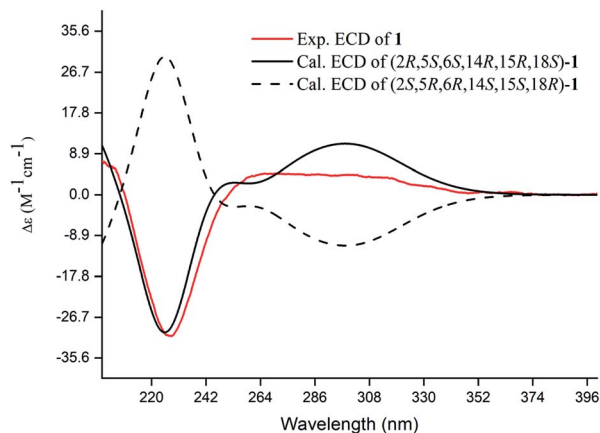


Fig. 4 Experimental and calculated ECD spectra of compound 1.

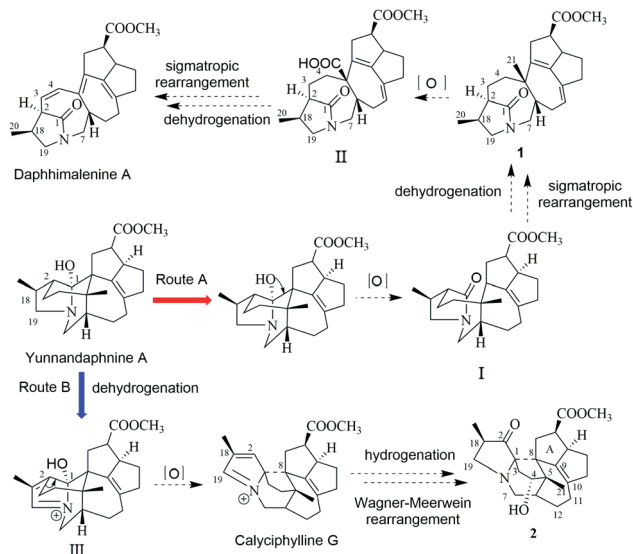
hydrogenation of  $\Delta_{2,18}/\Delta_{19,N}$  and oxidation of C-2 and C-4 result in the formation of 2.

Compound 3 has a molecular formula of  $C_{24}H_{33}O_4N$  with nine degrees of unsaturation. Analysis of spectroscopic data of 3 suggested that 3 have the same skeleton as that of calyciphylline E (11).<sup>16</sup> The major difference is the presence of an additional methoxy group in 3. Based on the HMBC correlation from *H*-methoxy ( $\delta_H$  3.25, s) to C-1 ( $\delta_C$  98.3), the methoxy group was placed at C-1 (Fig. 2). The NOESY correlations (Fig. 3) between *H*-methoxy to H-2/H-18 suggest that they are on the same side and assigned as an  $\alpha$ -orientation. Consequently, the structure of 3 was identified as shown in Fig. 1, and named calycindaphine C.

The molecular formula of compound 4 was deduced as  $C_{22}H_{29}O_4N$  on the basis of its HRESIMS data. The NMR spectroscopic data of 4 were closely related to that of oldhamiphylline A<sup>17</sup> except that the hydroxylated methine at  $\delta_C$  75.8, the methylene at  $\delta_C$  37.1, and the *N*-substituted methylene at  $\delta_C$  61.34 in oldhamiphylline A are replaced by a methylene at  $\delta_C$  25.4 (C-11), a hydroxylated quaternary carbon at  $\delta_C$  77.4 (C-18), and a lactam carbonyl carbon at  $\delta_C$  174.4 (C-19) in 4, respectively. These changes were proved by the HMBC correlations from H-10/H-12 to C-11, H-1/H-2/H-3/H-20 to C-18, and H-1/H-7/H-20 to C-19 (Fig. 2). The significant NOESY cross-peak of H-21/H-1 demonstrated the H-21 and H-1 were cofacial and placed C-21 to  $\alpha$ -orientation (Fig. 3). Furthermore, the NOESY correlation from H-20 to H-3 indicated there are on the same side and placed C-20 to  $\beta$ -orientation. Accordingly, the hydroxyl group attaching to C-18 was assigned as  $\beta$ -orientation. Therefore, the structure of 4 was identified as shown in Fig. 1, and named calycindaphine D.

Calycindaphines E–G (5–7) possess the molecular formula  $C_{23}H_{33}O_4N$ ,  $C_{23}H_{31}O_5N$ , and  $C_{23}H_{31}O_4N$ , respectively. Their NMR data analysis suggested that compounds 5–7 belong to daphnezomine F-type skeleton.<sup>18</sup> The NMR data of 5 are similar to those of daphlongeranine C<sup>18</sup> except that the hydroxy methylene at C-21 in daphlongeranine C was replaced by a singlet methyl in 5. This change was supported by the HMBC correlations from H-21 to C-4/C-5/C-6/C-8 and H-4/H-6 to C-5/C-21. Compound 6 is structurally like 5 except that the C-9/C-10





Scheme 1 Biogenetic pathway proposed for compounds 1 and 2, daphhimalenine A, and calyciphylline G.

double bond, the methylene at C-7, and the *O*-methine at C-2 in 5 are absent in 6, and an acylamide, two oxygenated quaternary carbons, and a methylene were presented in 6, respectively. The oxygenated C-9/C-10 in 6 were devised as an epoxy three-membered ring by the chemical shifts of C-9 and C-10 combined with the exclusive molecular formula from the exact result of HRESIMS. In addition, the HMBC correlations from H-6/H-12/H-19 to the extra acylamide (C-7), H-15/H-16/H-17 to the pair of oxygenated quaternary carbons (C-9/C-10), and H-20/H-18/H-4/H-3 to C-2 supported the above conjectures. Comparison of the chemical shifts of C-9 and C-10 with those of alkaloids containing epoxy group at C-9 and C-10 suggested that the epoxy group in 6 is  $\alpha$ -oriented.<sup>19–21</sup> Careful analysis of NMR data of 7 indicated that 7 is a daphnezomine F-type alkaloid with two double bonds and a hydroxylated quaternary carbon. HMBC correlations from H-7 to C-1/C-5/C-6/C-12/C-19, H-4/H-12/H-21 to C-6, H-15/H-16/H-11 to C-10/C-17, and H-14/H-15 to C-9 implied that two double bonds were placed at C-7/C-6 and C-10/C-17, and the hydroxylated quaternary carbon was fixed at C-9. Thus, the structures of 5–7 were determined as shown (Fig. 1).

The 1D NMR data of 8 suggested that compound 8 was closely related to 23.<sup>11</sup> The major differences between 8 and 23 were that the chemical shift of H-22 was down-shielded from  $\delta_{\text{H}}$  3.33 (in 23) to  $\delta_{\text{H}}$  3.94 (in 8), which might be caused by the different configuration of C-22. Furthermore, analysis of the <sup>1</sup>H–<sup>1</sup>H COSY and HMBC spectra implied that 8 and 23 have same planar structure. The NOESY cross-peak (Fig. 3) between H-22/H-24 in 8 illustrating that these protons are in cofacial and assigned to be  $\beta$ -orientation, which is opposite to that of 23. Furthermore, the optical value of 8 and 23 was measured as  $[\alpha]_{\text{D}}^{22.5} +26.8$  ( $c = 0.5$ , MeOH) and  $[\alpha]_{\text{D}}^{22.5} -49.4$  ( $c = 0.5$ , MeOH) respectively, which also provided evidence for the different configuration of C-22 in 8 and 23. Accordingly, compound 8 was elucidated as shown in Fig. 1 and named calycindaphnine H.

Calycindaphnine I (9) has a molecular formula C<sub>30</sub>H<sub>47</sub>O<sub>4</sub>N. Comparison of its 1D NMR spectra with those of 8 showed that the hydroxylated methine at  $\delta_{\text{C}}$  75.5 (C-22) and methyl at  $\delta_{\text{C}}$  21.3 (C-21) in 8 are replaced by a carbonyl at  $\delta_{\text{C}}$  213.0 (C-22) and a hydroxylated methylene carbon at  $\delta_{\text{C}}$  66.2 (C-21) in 9, respectively. These changes were further confirmed by the HMBC correlations from H-21 to C-4/C-5/C-6/C-8 and H-13/H-14/H-24 to C-22 (Fig. 2). Thus, the structure of 9 was determined as shown in Fig. 1.

Compound 10 showed a protonated  $[M + H]^+$  molecular ion at  $m/z$  474.3958, corresponding to a molecular formula of C<sub>30</sub>H<sub>51</sub>O<sub>3</sub>N, with six indices of hydrogen deficiency. The 1D NMR data of 10 are similar to those of daphnioldhanine F,<sup>22</sup> except that the characteristic hemiacetal carbon at C-25 in daphnioldhanine F was replaced by an oxidized methylene [ $\delta_{\text{C}}$  72.0, and  $\delta_{\text{H}}$  3.65 (m), 3.49 (d,  $J = 10.3$  Hz)] in 10. The HMBC correlations (Fig. 3) from H-25 to C-22/C-23/C-24 and H-24 to C-22/C-23/C-25/C-26 confirmed the assignment. The data of HRESIMS suggested that 10 has one less degree of unsaturation and a more H<sub>2</sub>O unit than that of the daphnioldhanine F. The chemical shift of C-29 in 10 appears in upfield shift (*ca.* 11 ppm) than the similar alkaloids possessing the linkage C-25–O–C-

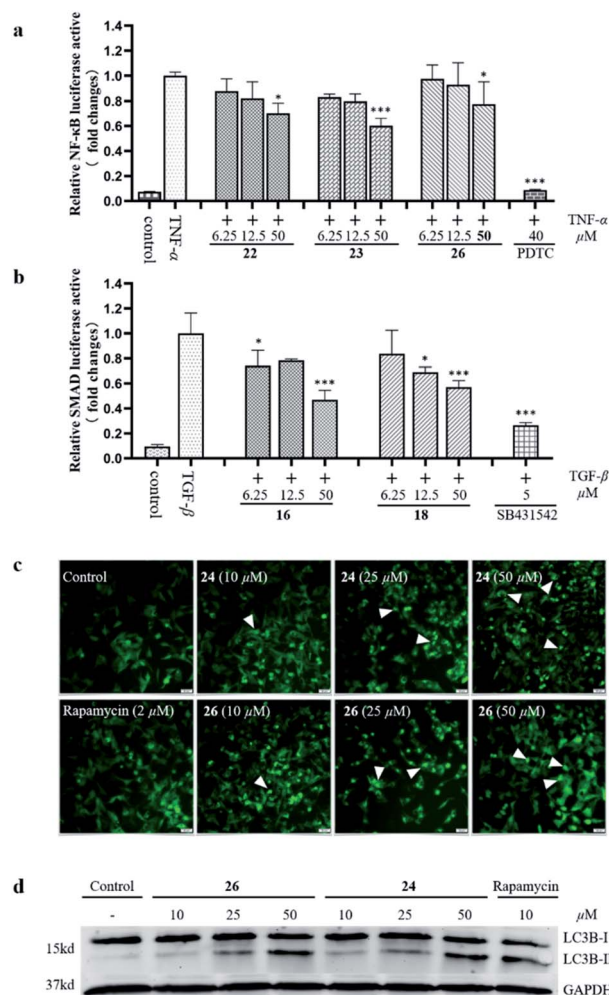


Fig. 5 The effects of isolated alkaloids on TNF $\alpha$ -induced NF- $\kappa$ B activation (a), TGF- $\beta$ /SMAD pathway (b), and cell autophagy (c and d).



29,<sup>22,23</sup> which supported that the specific linkage of C-25–O–C-29 in secodaphniphylline-type alkaloids is broken to form a hydroxy at C-25 and C-29 in **10**, respectively. The above spectroscopic evidence deduced the structure of **10** as depicted in Fig. 1, and named calycindaphine J.

By NMR data analysis and comparison of the reported spectroscopic data, 17 known compounds (**11**–**27**) were identified as calyciphylline E (**11**),<sup>16</sup> calyciphylline Q (**12**),<sup>24</sup> yunnan-daphnine A (**13**),<sup>7</sup> macrodaphniphyllamine (**14**),<sup>7</sup> yunnandaphnine E (**15**),<sup>7</sup> caldaphnidine A (**16**),<sup>11</sup> (–)-bukittinggine (**17**),<sup>25</sup> longistylumphylline C (**18**),<sup>26</sup> deoxyisocalyciphylline B (**19**),<sup>27</sup> deoxycalyciphylline B (**20**),<sup>25,27</sup> caldaphnidine D (**21**),<sup>11</sup> secodaphniphylline (**22**),<sup>28</sup> caldaphnidine E (**23**),<sup>11</sup> daphnioldhanin G (**24**),<sup>22</sup> daphnioldhanin D (**25**),<sup>29</sup> daphnioldhanin E (**26**),<sup>22</sup> and calyciphylline D (**27**).<sup>30</sup>

Previous phytochemical studies have shown that *Daphniphyllum* alkaloids from *D. calycinum* mainly focused on the anti-cancer effect.<sup>15,31</sup> But, in the traditional folk medicine, the plants of *D. calycinum* are extensively used to treat different diseases which are closely related to inflammation.<sup>11–13</sup> To provide more evidences for the pharmacological action of alkaloids from *D. calycinum*, all isolated alkaloids were evaluated for their effects on TNF $\alpha$ -induced NF- $\kappa$ B activation, TGF- $\beta$  pathway, and cell autophagy. The bioassay results showed that compounds **22**, **23**, and **26** inhibited TNF $\alpha$ -induced NF- $\kappa$ B activation in a dose dependent manner (Fig. 5a). Compounds **16** and **18** exhibited significant inhibitory activity on TGF- $\beta$ /SMAD pathway at a concentration of 50  $\mu$ M in HepG2 cells (Fig. 5b). Two compounds (**24** and **26**) revealed their autophagy modulating activities by inducing autophagic puncta and upregulating the autophagy marker LC3-II levels in HEK293 cells (Fig. 5c/d).

## Conclusions

In conclusion, ten new *Daphniphyllum* alkaloids, calycindaphines A–J (**1**–**10**), together with 17 known alkaloids were isolated from the roots of *D. calycinum*. Compound **1** is a novel alkaloid with a new C<sub>22</sub> skeleton with a rare 5/8/7/5/5 ring system containing a unique 1-azabicyclo[5.2.1]decane. Compound **2** is the second example for the unique skeleton with 5/6/5/8/5/5 ring system. Compound **10** is the first example of secodaphniphylline-type alkaloid absent of the oxygen-bridge between C-25/C-29.

Compounds **16**, **18**, **22**–**24**, and **26** exhibited their potential bioactivities on NF- $\kappa$ B or TGF- $\beta$  inhibition and/or cell autophagic induction. Our findings not only revealed the chemicals from the roots of *D. calycinum* for the first time, but also give a new insight into the complex polycyclic skeletons and structural diversity of *Daphniphyllum* alkaloids.

## Experimental section

### General experimental procedures

Optical rotations were measured on a Rudolph Research Analytical Autopol I automatic polarimeter. Ultraviolet (UV) and CD spectra were recorded on a Jasco J-1500 Circular Dichroism Spectrometer. IR spectra were carried on an Agilent Cary 660

series FT-IR spectrometer (KBr). HRESIMS spectra were obtained on an Agilent 6230 HRESIMS spectrometer. 1D and 2D NMR spectra were performed on a Bruker Ascend 600 NMR spectrometer. The chemical shifts were expressed in  $\delta$  (ppm) with TMS as an internal reference. Column chromatography was performed on Silica gel (40–60 mesh, Grace, USA) column. Thin layer chromatography was carried on precoated silica gel 60 F<sub>254</sub> plates (200  $\mu$ m thick, Merck KGaA, Germany). MPLC was performed using a Buchi Sepacore flash system with a RP-18 column (SilicBond C<sub>18</sub>, 36  $\times$  460 mm ID, 40–63  $\mu$ m particle size). Semi-preparative HPLC was conducted on an Agilent 1100/1200 liquid chromatography instrument with a Waters Xbridge Prep C<sub>18</sub> column (10  $\times$  250 mm, 5  $\mu$ m) or Xbridge Prep C<sub>8</sub> column (10  $\times$  250 mm, 5  $\mu$ m). UHPLC analyses were conducted on an Agilent 1290 system using a ZORBAX RRHD Eclipse Plus C<sub>18</sub> column (1.8  $\mu$ m, 2.1  $\times$  50 mm, Agilent).

### Plant material

The roots of *D. calycinum* were collected from Guigang city of Guangxi Province, People's Republic of China, in October 2018, and identified by one of the authors, Dr Zhu G.-Y. A voucher specimen (DC-201810) was deposited at State Key Laboratory of Quality Research in Chinese Medicine, Macau University of Science and Technology.

### Extraction and isolation

The air-dried, powdered roots (30 kg) of *D. calycinum* were extracted three times with 80% EtOH. The combined filtrates were concentrated under vacuum to afford a dark extract, which was adjusted to pH 2 with HCl. The acidic mixture was centrifuged to remove dark brown precipitates. The aqueous layer was basified to pH 10 with NaHCO<sub>3</sub> and then exhaustively extracted with EtOAc to afford the crude alkaloids (170.0 g). The crude alkaloids were subjected to a Silica gel column (CHCl<sub>3</sub>/MeOH, 1 : 0–0 : 1) to obtain 10 fractions (Fr.A–Fr.F).

Fr.A (22.5 g) was further chromatographed on a silica gel (40–60 mesh) column (CHCl<sub>3</sub>/MeOH, 1 : 0–1 : 20) to give 10 sub-fractions (Fr.A1–Fr.A10). Compounds **16** (560.0 mg) and **17** (11.0 mg) were isolated and purified by semipreparative reversed-phase (RP) HPLC with C-18 column eluted with 75% MeCN/0.1% DEA from the fraction Fr.A1. The fraction Fr.A2 was separated into two subfractions (Fr.A2a and Fr.A2b) by MPLC on C-18 column eluting with a gradient of MeCN/0.1% DEA–H<sub>2</sub>O (20 : 80 to 100 : 0, v/v). Fr.A2a was subjected to RP-HPLC with C-18 column (75% MeCN/0.1% DEA) to obtain **4** (6.2 mg). Fr.A2b was purified by semi-preparative HPLC with 72% MeCN/0.1% DEA to give **5** (29.0 mg) and **6** (5.2 mg). Fr.A3 was submitted to CC on silica gel to yield the subfraction (Fr.A3a). Fr.A3a was further purified by RP-HPLC with C-8 column eluted with 80% MeCN/0.1% DEA to afford **18** (95.0 mg), **24** (11.1 mg), **25** (11.0 mg), and **26** (35.0 mg). Fr.A4 was purified by semi-preparative HPLC with a C-18 column to give **22** (88.0 mg). Compound **27** (24.0 mg) was acquired by means of recrystallization from Fr.A10.

Fr.B (20.1 g) was subjected to MPLC on C-18 column and eluted with a gradient of MeCN/0.1% DEA–H<sub>2</sub>O (20 : 80 to



100 : 0, v/v) to give four subfractions (Fr.B1–Fr.B4). Fr.B1 was isolated by semi-preparative HPLC with C-18 column (60% MeCN/0.1% DEA) to obtain three alkaloids, **2** (3.6 mg), **19** (76.8 mg), and **20** (16.3 mg). Fr.B2 was separated by RP-HPLC with C-18 column (75% MeCN/0.1% DEA) to yield Fr.B2a and Fr.B2b. Fr.B2a was purified by RP-HPLC with C-18 column (54% MeCN/0.1% DEA) to give **7** (3.1 mg). Fr.B2b was purified by RP-HPLC (62% MeCN/0.1% DEA) to give **1** (7.0 mg). Fr.B3 was isolated by RP-HPLC with C-8 column (65% MeCN/0.1% DEA) to yield **13** (15.7 mg). Fr.C (19.3 g) was isolated by the MPLC on C-18 to give Fr.C8 and then was purified by RP-HPLC with C-18 column (55% MeCN/0.1% DEA) to afford **12** (2.6 mg). Fr.D (9.2 g) was separated by MPLC with a C-18 column and eluted with a gradient of MeCN/0.1% DEA–H<sub>2</sub>O (10 : 80 to 100 : 0, v/v) to give the main subfraction of Fr.D1. And then, the subfraction was separated by the RP-HPLC with C-18 column (58% MeCN/0.1% DEA) to afford **3** (2.5 mg), **9** (4.0 mg), **11** (16.0 mg), **14** (3.6 mg), **15** (45.0 mg), **21** (6.2 mg), and **23** (22.0 mg). Alkaloids of Fr.F (6.0 g) were enriched by the MPLC to give the main subfraction Fr.F7 which was purified by RP-HPLC with C-18 column to obtain **8** (2.7 mg) and **10** (5.2 mg).

**Calycindaphine A (1).** White amorphous powder;  $[\alpha]_{\text{D}}^{22.5} -12.5$  ( $c = 0.5$ , MeOH); UV (MeOH)  $\lambda_{\text{max}}$  (log  $\epsilon$ ): 200.4 (7.45), 304.8 (0.620) nm; IR (KBr)  $\nu_{\text{max}}$ : 3730, 3700, 3625, 3595, 3444, 2956, 1768, 1708, 1448, 1388, 1266, 1200, 754  $\text{cm}^{-1}$ ; ECD (MeOH)  $\lambda_{\text{max}}$  (log  $\epsilon$ ): 217.2 (–51.89), 270.6 (32.30), 352.2 (–36.27) nm; <sup>1</sup>H NMR and <sup>13</sup>C NMR see Tables 1 and 2; HRESIMS  $m/z$  370.2340  $[\text{M} + \text{H}]^+$  (calcd for C<sub>23</sub>H<sub>31</sub>NO<sub>4</sub> 370.2375).

**Calycindaphine B (2).** White amorphous powder;  $[\alpha]_{\text{D}}^{22.5} -39.8$  ( $c = 0.5$ , MeOH); UV (MeOH)  $\lambda_{\text{max}}$  (log  $\epsilon$ ): 201.1 (6.66), 346.1 (1.24) nm; IR (KBr)  $\nu_{\text{max}}$ : 3730, 3595, 3442, 2929, 1733, 1645, 1562, 1442, 1387, 1268, 1169, 754  $\text{cm}^{-1}$ ; ECD (MeOH)  $\lambda_{\text{max}}$  (log  $\epsilon$ ): 200.4 (–52.76), 226.8 (166.29) nm; <sup>1</sup>H NMR and <sup>13</sup>C NMR see Tables 1 and 2; HRESIMS  $m/z$  386.2324  $[\text{M} + \text{H}]^+$  (calcd for C<sub>23</sub>H<sub>32</sub>NO<sub>4</sub> 386.2326).

**Calycindaphine C (3).** White amorphous powder;  $[\alpha]_{\text{D}}^{22.5} -52.9$  ( $c = 0.5$ , MeOH); UV (MeOH)  $\lambda_{\text{max}}$  (log  $\epsilon$ ): 201.3 (1.26), 304.8 (0.66) nm; IR (KBr)  $\nu_{\text{max}}$ : 3730, 3701, 3626, 3596, 3449, 2933, 2865, 1735, 1649, 1545, 1393, 1358, 756  $\text{cm}^{-1}$ ; ECD (MeOH)  $\lambda_{\text{max}}$  (log  $\epsilon$ ): 214.2 (–33.48), 247.8 (5.28), 283.2 (–13.25) nm; <sup>1</sup>H NMR and <sup>13</sup>C NMR see Tables 1 and 2; HRESIMS  $m/z$  400.3485  $[\text{M} + \text{H}]^+$  (calcd for C<sub>24</sub>H<sub>34</sub>NO<sub>4</sub> 400.2482).

**Calycindaphine D (4).** White amorphous powder;  $[\alpha]_{\text{D}}^{22.5} -41.5$  ( $c = 0.5$ , MeOH); UV (MeOH)  $\lambda_{\text{max}}$  (log  $\epsilon$ ): 199.5 (12.9) nm; IR (KBr)  $\nu_{\text{max}}$ : 3730, 3701, 3625, 3596, 3380, 2949, 2858, 1770, 1699, 1546, 1425, 1388, 1350, 1268, 1128, 1093, 1043, 754  $\text{cm}^{-1}$ ; ECD (MeOH)  $\lambda_{\text{max}}$  (log  $\epsilon$ ): 209.5 (533.12), 230.2 (–181.22) nm; <sup>1</sup>H NMR and <sup>13</sup>C NMR see Tables 1 and 2; HRESIMS  $m/z$  372.2166  $[\text{M} + \text{H}]^+$  (calcd for C<sub>22</sub>H<sub>30</sub>NO<sub>4</sub> 372.2169).

**Calycindaphine E (5).** White amorphous powder;  $[\alpha]_{\text{D}}^{22.5} -40.5$  ( $c = 0.5$ , MeOH); UV (MeOH)  $\lambda_{\text{max}}$  (log  $\epsilon$ ): 204.1 (8.95) nm; IR (KBr)  $\nu_{\text{max}}$ : 3730, 3701, 3625, 3595, 3426, 2929, 1730, 1650, 1484, 1434, 1355, 1316, 1280, 1170, 1036, 741  $\text{cm}^{-1}$ ; ECD (MeOH)  $\lambda_{\text{max}}$  (log  $\epsilon$ ): 205.2 (271.64), 230.4 (–310.91) nm; <sup>1</sup>H NMR and <sup>13</sup>C NMR see Tables 1 and 2; HRESIMS  $m/z$  388.2480  $[\text{M} + \text{H}]^+$  (calcd for C<sub>23</sub>H<sub>34</sub>NO<sub>4</sub> 388.2482).

**Calycindaphine F (6).** White amorphous powder;  $[\alpha]_{\text{D}}^{22.5} -26.3$  ( $c = 0.5$ , MeOH); UV (MeOH)  $\lambda_{\text{max}}$  (log  $\epsilon$ ): 200.7 (4.12), 222.8 (6.62) nm; IR (KBr)  $\nu_{\text{max}}$ : 3730, 3701, 3625, 3595, 3446, 2927, 2875, 1725, 1680, 1447, 1380, 1270, 1173, 755  $\text{cm}^{-1}$ ; ECD (MeOH)  $\lambda_{\text{max}}$  (log  $\epsilon$ ): 229.1 (–413.27), 256.8 (72.60) nm; <sup>1</sup>H NMR and <sup>13</sup>C NMR see Tables 1 and 2; HRESIMS  $m/z$  402.2293  $[\text{M} + \text{H}]^+$  (calcd for C<sub>23</sub>H<sub>32</sub>NO<sub>5</sub> 402.2275).

**Calycindaphine G (7).** White amorphous powder;  $[\alpha]_{\text{D}}^{22.5} -57.0$  ( $c = 0.5$ , MeOH); UV (MeOH)  $\lambda_{\text{max}}$  (log  $\epsilon$ ): 202.4 (4.54), 264.8 (1.03) nm; IR (KBr)  $\nu_{\text{max}}$ : 3730, 3701, 3626, 3596, 3446, 3927, 1731, 1644, 1457, 1391, 1271, 755  $\text{cm}^{-1}$ ; ECD (MeOH)  $\lambda_{\text{max}}$  (log  $\epsilon$ ): 198.0 (–217.81), 234.6 (68.96), 264.0 (–150.08) nm; <sup>1</sup>H NMR and <sup>13</sup>C NMR see Tables 1 and 2; HRESIMS  $m/z$  386.2332  $[\text{M} + \text{H}]^+$  (calcd for C<sub>23</sub>H<sub>32</sub>NO<sub>4</sub> 386.2326).

**Calycindaphine H (8).** White amorphous powder;  $[\alpha]_{\text{D}}^{22.5} +26.8$  ( $c = 0.5$ , MeOH); IR (KBr)  $\nu_{\text{max}}$ : 3866, 3730, 3701, 3620, 3596, 3447, 2926, 2863, 2379, 2316, 1697, 1650, 1570, 1549, 1518, 1385, 1055, 751, 464, 451  $\text{cm}^{-1}$ ; ECD (MeOH)  $\lambda_{\text{max}}$  (log  $\epsilon$ ): 223.2 (10.89), 265.8 (–14.92), 294.6 (–4.72), 313.2 (10.71) nm; <sup>1</sup>H NMR and <sup>13</sup>C NMR see Tables 1 and 2; HRESIMS  $m/z$  472.3786  $[\text{M} + \text{H}]^+$  (calcd C<sub>30</sub>H<sub>50</sub>NO<sub>3</sub> for 472.3785).

**Calycindaphine I (9).** White amorphous powder;  $[\alpha]_{\text{D}}^{22.5} -36.8$  ( $c = 0.5$ , MeOH); UV (MeOH)  $\lambda_{\text{max}}$  (log  $\epsilon$ ): 202.4 (3.28), 300.5 (1.76) nm; IR (KBr)  $\nu_{\text{max}}$ : 3730, 3701, 3625, 3595, 3446, 2934, 2868, 2316, 1703, 1647, 1545, 1458, 1392, 1268, 755  $\text{cm}^{-1}$ ; ECD (MeOH)  $\lambda_{\text{max}}$  (log  $\epsilon$ ): 210.6 (–29.16), 232.2 (–16.40), 288.6 (–16.97) nm; <sup>1</sup>H NMR and <sup>13</sup>C NMR see Tables 1 and 2; HRESIMS  $m/z$  486.3562  $[\text{M} + \text{H}]^+$  (calcd for C<sub>30</sub>H<sub>48</sub>NO<sub>4</sub> 486.3578).

**Calycindaphine J (10).** White amorphous powder;  $[\alpha]_{\text{D}}^{22.5} -33.7$  ( $c = 0.5$ , MeOH); IR (KBr)  $\nu_{\text{max}}$ : 3730, 3701, 3625, 3595, 3446, 2934, 2866, 1648, 1572, 1549, 1518, 1461, 1386, 1386, 1268, 1040, 752  $\text{cm}^{-1}$ ; <sup>1</sup>H NMR and <sup>13</sup>C NMR see Tables 1 and 2; HRESIMS  $m/z$  474.3958  $[\text{M} + \text{H}]^+$  (calcd for C<sub>30</sub>H<sub>52</sub>NO<sub>3</sub> 474.3942).

### ECD calculations of compound 1

Conformational analyses were carried out *via* random searching in the Sybyl-X 2.0 using the MMFF94S force field with an energy cutoff of 2.5 kcal mol<sup>–1</sup>. The results showed the nine lowest energy conformers for both compounds. Subsequently, the conformers were re-optimized using DFT at the PBE0-D3(BJ)/def2-SVP level in MeOH using the polarizable conductor calculation model (SMD) by the ORCA4.2.1 program. The energies, oscillator strengths, and rotational strengths (velocity) of the first 60 electronic excitations were calculated using the TDDFT methodology at the PBE0/def2-TZVP level in MeOH. The ECD spectra were simulated by the overlapping Gaussian function (half the bandwidth at 1/*e* peak height, sigma = 0.30 for all). To get the final spectra, the simulated spectra of the conformers were averaged according to the Boltzmann distribution theory and their relative Gibbs free energy ( $\Delta G$ ).

### Cell lines and cell cultures

The HepG2-NF- $\kappa$ B-Luc cell line is stably transfected with the NF- $\kappa$ B-luciferase gene, which was generously provided by Dr C. H.



Leung (University of Macau). Cells were cultivated with DMEM medium supplemented with 10% fetal bovine serum (FBS), 100 U mL<sup>-1</sup> penicillin, and 100 µg mL<sup>-1</sup> streptomycin at 37 °C with 5% CO<sub>2</sub> and 95% air incubator.

SMAD 2/3 responsive luciferase reporter HepG2 stable cell line was purchased from Signosis. Cells were cultivated with DMEM medium supplemented with 5% FBS, 100 U mL<sup>-1</sup> penicillin, 100 µg mL<sup>-1</sup> streptomycin, and 100 µg mL<sup>-1</sup> hygromycin B at 37 °C with 5% CO<sub>2</sub> and 95% air incubator.

HEK293 cell line stable transfected with GFP-LC3 was kindly provided by Dr X. M. Zhu (Macau University of Science and Technology). The cells were cultured in an  $\alpha$ -MEM medium supplemented with 10% FBS under a humidified atmosphere containing 5% CO<sub>2</sub> at 37 °C.

### NF- $\kappa$ B luciferase assay

The NF- $\kappa$ B activity was determined by NF- $\kappa$ B luciferase assay as described in our previous publication with a slight modification.<sup>32</sup> Briefly, HepG2-NF- $\kappa$ B-Luc cells were seeded on a 96-well microplate with  $1 \times 10^4$  cells per well and cultured at 37 °C with 5% CO<sub>2</sub> incubator for 18 h. Then, cells were pretreated with compounds (6, 12.5, and 50 µM) for 12 h and induced with TNF- $\alpha$  (10 ng mL<sup>-1</sup>) for 4 h. Ammonium pyrrolidinedithiocarbamate (PDTTC) was used as the positive control. The firefly luciferase signal was measured with the Bright-Glo Luciferase Reporter Assay System (Promega, Madison, WI) according to the manufacturer's instruction using a multimode reader (SpectraMax iD5, Danaher).

### TGF- $\beta$ induced SMAD luciferase assay

The effects of compounds on the TGF- $\beta$ /SMAD were determined by TGF- $\beta$ /SMAD luciferase assay. Briefly, HepG2/SMAD-Luc cells were seeded on a 96-well microplate with  $1 \times 10^4$  cells per well and cultured at 37 °C with 5% CO<sub>2</sub> incubator for 18 h. After adhesion, the cells were pretreated with compounds at different concentration for 6 h and induced with TGF- $\beta$  (10 ng mL<sup>-1</sup>) for 18 h. Meanwhile, SB-431542, a specific inhibitor of TGF- $\beta$  Receptor Kinase, was applied as the positive control. The firefly luciferase signal was measured with the Bright-Glo Luciferase Reporter Assay System (Promega, Madison, WI) according to the manufacturer's instruction using a multimode reader (SpectraMax iD5, Danaher).

### LC3 puncta counting

The HEK293-GFP-LC3 cells were applied for visualizing autophagosome formation after treatment with various compounds for 24 hours. During autophagosome formation, GFP-LC3 is processed and recruited to the autophagosome membrane, where it can be imaged as cytoplasmic puncta by IncuCyte ZOOM live cell imaging (Olympus, coupled with Hamama Tsu ORCA-Flash 40 LT Plus Scientific CMOS Digital Camera). The percentage of GFP-LC3 positive cells can be determined and is indicative of autophagosome formation.

### Western blot analysis

Primary antibody against LC3II was purchased from Cell Signaling Technology. Primary antibody against glyceraldehyde-3-phosphate dehydrogenase (GAPDH) was purchased from Abcam Inc. (Cambridge, MA). Secondary antibodies, and goat anti-mouse/anti-rabbit IgG H&L (IRDye 800CW) were purchased from Abcam Inc. (Cambridge, MA).

The cells were seeded onto 6-well plates with  $\alpha$ -MEM medium and cultured for 24 hours. After treating with various concentrations of compounds 24 and 26, cells were collected and lysed in lysis buffer on ice for 30 minutes. Protein samples were electrophoresed using 15% SDS-PAGE gel and transferred onto a nitrocellulose membrane (NC membrane). The membranes were blocked by a 5% BSA and incubated with the primary antibody overnight at 4 °C, followed by the secondary antibody for 1 hour at room temperature. Protein bands were detected by the LI-COR Odyssey imaging system (Lincoln, NE).

### Conflicts of interest

There are no conflicts to declare.

### Acknowledgements

This work was financially supported by the Macao Science and Technology Development Funds (0008/2019/A, 0075/2019/AGJ, 0023/2019/AKP, and 125/2017/A3).

### Notes and references

- 1 S. Yamamura, H. Irikawa, Y. Okumura and Y. Hirata, *Bull. Chem. Soc. Jpn.*, 1975, **48**, 2120–2123.
- 2 J. i. Kobayashi and T. Kubota, *Nat. Prod. Rep.*, 2009, **26**, 936–962.
- 3 M. Cao, Y. Zhang, H. He, S. Li, S. Huang, D. Chen, G. Tang, S. Li, Y. Di and X. Hao, *J. Nat. Prod.*, 2012, **75**, 1076–1082.
- 4 M.-M. Cao, L. Wang, Y. Zhang, H.-P. He, Y.-C. Gu, Q. Zhang, Y. Li, C.-M. Yuan, S.-L. Li and Y.-T. Di, *Fitoterapia*, 2013, **89**, 205–209.
- 5 H. Wu, X. Zhang, L. Ding, S. Chen, J. Yang and X. Xu, *Planta Med.*, 2013, **79**, 1589–1598.
- 6 T. Nakano, M. Hasegawa and Y. Saeki, *J. Org. Chem.*, 1973, **38**, 2404–2405.
- 7 Y.-T. Di, H.-P. He, C.-S. Li, J.-M. Tian, S.-Z. Mu, S.-L. Li, S. Gao and X.-J. Hao, *J. Nat. Prod.*, 2006, **69**, 1745–1748.
- 8 H. Morita and J. i. Kobayashi, *Org. Lett.*, 2003, **5**, 2895–2898.
- 9 G. A. Wallace and C. H. Heathcock, *J. Org. Chem.*, 2001, **66**, 450–454.
- 10 T. He, Y. Zhou, Y. H. Wang, S. Z. Mu and X. J. Hao, *Helv. Chim. Acta*, 2011, **94**, 1019–1023.
- 11 Z.-J. Zhan, C.-R. Zhang and J.-M. Yue, *Tetrahedron*, 2005, **61**, 11038–11045.
- 12 C.-R. Zhang, S.-P. Yang and J.-M. Yue, *J. Nat. Prod.*, 2008, **71**, 1663–1668.
- 13 S.-M. Shen, H. Li, J.-R. Wang, Y.-B. Zeng and Y.-W. Guo, *Tetrahedron*, 2020, 131616.



- 14 Y. Zhang, Y.-T. Di, Q. Zhang, S.-Z. Mu, C.-J. Tan, X. Fang, H.-P. He, S.-L. Li and X.-J. Hao, *Org. Lett.*, 2009, **11**, 5414–5417.
- 15 S. Saito, T. Kubota and J. i. Kobayashi, *ChemInform*, 2007, **48**, 5693–5695.
- 16 S. Saito, T. Kubota and J. i. Kobayashi, *Tetrahedron Lett.*, 2007, **48**, 3809–3812.
- 17 X. Chen, Z. J. Zhan and J. M. Yue, *Chem. Biodiversity*, 2004, **1**, 1513–1518.
- 18 T. Q. Yang, Y. T. Di, H. P. He, Q. Zhang, Y. Zhang and X. J. Hao, *Helv. Chim. Acta*, 2011, **94**, 397–403.
- 19 C. R. Zhang, H. B. Liu, S. H. Dong, J. Y. Zhu, Y. Wu and J. M. Yue, *Org. Lett.*, 2009, **11**, 4692–4695.
- 20 C. S. Li, Y. T. Di, S. Z. Mu, H. P. He and X. J. Hao, *J. Nat. Prod.*, 2008, **71**, 1202–1206.
- 21 Z. Li, S. Peng, L. Fang, Y. Yang and Y. Guo, *Chem. Biodiversity*, 2010, **6**, 105–110.
- 22 S. Z. Mu, X. W. Yang, Y. T. Di, H. P. He, Y. Wang, Y. H. Wang, L. Li and X. J. Hao, *Chem. Biodiversity*, 2007, **4**, 129–138.
- 23 S.-Z. Mu, J.-S. Wang, X.-S. Yang, H.-P. He, C.-S. Li, Y.-T. Di, Y. Wang, Y. Zhang, X. Fang and L.-J. Huang, *J. Nat. Prod.*, 2008, **71**, 564–569.
- 24 H. Yahata, T. Kubota and J. i. Kobayashi, *J. Nat. Prod.*, 2009, **72**, 148–151.
- 25 D. Arbain, L. Byrne, J. Cannon, V. Patrick and A. White, *Aust. J. Chem.*, 1990, **43**, 185–190.
- 26 X. Chen, Z. J. Zhan and J. M. Yue, *Helv. Chim. Acta*, 2005, **88**, 854–860.
- 27 X. Zhang, J. Zhang, Y. Tan, Q. Liu and M. Liu, *Molecules*, 2012, **17**, 9641–9651.
- 28 M. Toda, Y. Hirata and S. Yamamura, *Tetrahedron*, 1972, **28**, 1477–1484.
- 29 Z. J. Zhan, G. W. Rao, X. R. Hou, C. P. Li and W. G. Shan, *Helv. Chim. Acta*, 2009, **92**, 1562–1567.
- 30 S. Saito, T. Kubota, E. Fukushi, J. Kawabata, H. Zhang and J. i. Kobayashi, *Org. Lett.*, 2007, **9**, 1207–1209.
- 31 S. Saito, H. Yahata, T. Kubota, Y. Obara and J. I. Kobayashi, *Tetrahedron*, 2008, **64**, 1901–1908.
- 32 G.-Y. Zhu, L.-P. Bai, L. Liu and Z.-H. Jiang, *Phytochemistry*, 2014, **107**, 175–181.

